Phytochemistry 174 (2020) 112359

Contents lists available at ScienceDirect

Phytochemistry

journal homepage: www.elsevier.com/locate/phytochem

Study of two isoforms of lipoxygenase by kinetic assays, docking and molecular dynamics of a specialised metabolite isolated from the aerial portion of *Lithrea caustica* (Anacardiaceae) and its synthetic analogs

Alejandra Muñoz-Ramírez**, Claudia Torrent-Farías, Carolina Mascayano-Collado*, Alejandro Urzúa-Moll

Departamento de Ciencias Del Ambiente, Facultad de Química y Biología, Universidad de Santiago, Chile, Casilla 442, Correo 2, Santiago, Chile

ARTICLE INFO

Keywords:
Lithrea caustica
Anacardiaceae
Natural products
5-LOX inhibition
Anticancer agents
Molecular dynamics

ABSTRACT

Our investigation focused on the characterization and study of epicuticular leaf extracts (dichloromethane extract) and certain derivatives of *Lithrea caustica* (Molina) Hook and Arn. (Anacardiaceae) as inhibitors of 15 soybean and 5 human lipoxygenases (15-sLOX and 5-hLOX). From the epicuticular extract of leaves, the compound (*Z*)-3-(pentadec-10′-enyl)-catechol (*Litreol*) was isolated, and three hemisynthetic derivatives were prepared, as they are 3-pentadecylcatechol, (*Z*)-1,2-diacetyl-3-(pentadec-10′-enyl)-benzene and 1,2-diacetyl-3-pentadecylbenzene. The inhibitory activities for the four compounds against 15-sLOX and 5-hLOX were determined, being (*Z*)-3-(pentadec-10′-enyl)-catechol (IC_{50} 54.77 μM and 2.09 μM, respectively) and 3-pentadecylcatechol (IC_{50} 55.28 μM and 2.74 μM, respectively), the most interesting compounds assayed. The kinetic studies for (*Z*)-3-(pentadec-10′-enyl)-catechol and 3-pentadecylcatechol showed a mixed inhibition mechanism to 5-LOX. Finally, docking and molecular dynamics studies were performed to characterize and describe how the chemical structures could be correlated to the decreased 5-hLOX activity observed in the *in vitro* studies.

1. Introduction

The Anacardiaceae family consists of approximately 68 genera and 600 species, among which are trees, shrubs and lianas of wide distribution from mostly tropical climates (Perrotta and Arambarri, 2004). Some species of Anacardiaceae are recognized for synthesizing a characteristic group of compounds, shown varied biological properties, including allergenic, antibacterial, fungicidal, antitumor, anti-inflammatory activities, etc. (Russo et al., 2009; Diby et al., 2016). These compounds constitute a family of lipophilic molecules that share a general structure, a catechol group at position 3 is substituted with one chain of 10, 12, 14, 15 or 17 carbon atoms, with one or more positions of unsaturation in the main chain, forming a complex mixture of alkylcatechols with very similar physicochemical properties (Kalergis et al., 1997; Aziz et al., 2017). For example, “urushiol”, an alkylcatechol (see Fig. 1), are a group of alkyls catechol that differing in the length and number of unsaturations of their alkyl chain (Gambaro et al., 1986) and are known to cause irritation, inflammation and blisters on the skin (Huang et al., 2018).

Some species of the Anacardiaceae family, which cause contact dermatitis, also contain anti-inflammatory compounds. These species include *Mangifera indica* L. (mango) (Garro et al., 2015) and species of the genus *Lithraea* (Alé et al., 1997).

The genus *Lithraea* is represented by four species distributed across Australia and the Americas. Three South American species (*L. caustica*, *L. molleoides* and *L. brasiliensis*) are known to produce allergic contact dermatitis (ACD) (Gambaro et al., 1986; López et al., 1998).

L. caustica (Molina) Hook. And Arn. (Anacardiaceae), commonly known as “litre”, is an evergreen tree, shrub or creeping plant that ranges from 0.5 to 3 m tall, is endemic to Chile (Huang et al., 2018; Teillier et al., 2018).

A study of the stem bark and leaves of *L. caustica* was carried out, and an alkylcatechol was isolated, commonly called “litreol”, whose structure was determined as 3-(pentadec-10′-enyl)-catechol (Gambaro et al., 1986) and is associated with the allergy produced by the litre (López et al., 1998).

In 2011, the study of epicuticular components of two populations of *L. caustica* by extracting fresh leaves using dichloromethane was performed. The extracts exhibited a mixture of n-alkanes of 21–33 carbon units as their main components and small levels of monoterpene

* Corresponding author.
** Corresponding author.
E-mail addresses: alejandra.munozr@usach.cl (A. Muñoz-Ramírez), carolina.mascayano@usach.cl (C. Mascayano-Collado).

https://doi.org/10.1016/j.phytochem.2020.112359
Received 23 May 2019; Received in revised form 17 March 2020; Accepted 18 March 2020

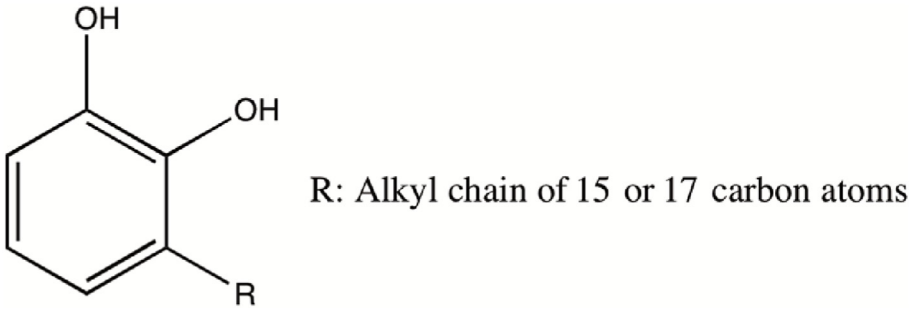

Fig. 1. Basic structure of urushiol.

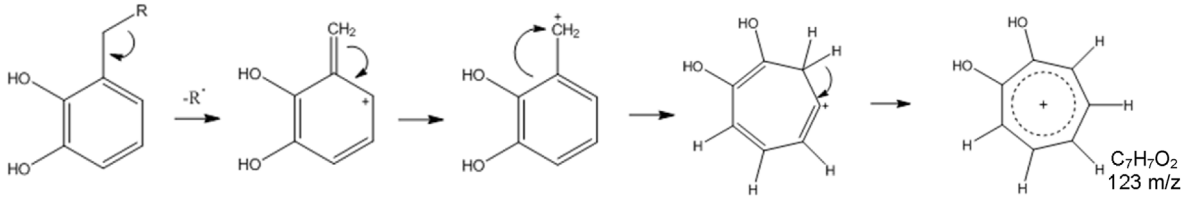

Fig. 2. Formation of tropylium ion with two phenolic –OH groups.

hydrocarbons in addition to the presence of 3-(pentadec-10′-enyl)-catechol, demonstrating that it is found in the epicuticle (Urzúa et al., 2011).

In folk medicine, the tincture of leaves is applied at homeopathic doses for squamous diseases of the skin, the leaves are eaten raw to avoid allergy problems (San Martín, 1983) and the stem juice of *L. caustica* with *Rubus ulmifolius* (blackberry) is used to treat coughs (Russo et al., 2009). Additionally, in Mapuche medicine, an infusion of leaves is used for parts of the body presenting with articular inflammations, which are submerged in the infusion (Gusinde, 1936; Montecino and Conejeros, 1985).

Inflammation protects the body against infections and injuries, but the response can cause various diseases, such as rheumatoid arthritis and inflammation of the intestine and psoriasis, among others.

LOXs regulate the pathophysiology of various diseases (Yar et al., 2014), also play an essential role in the biosynthesis of lipoxins (LX), thromboxanes (TX) and leukotrienes (LT) that generate the physiologically active oxygenated fatty acids (Nikolaev et al., 1990; Li et al., 2015; Imai et al., 2016).

The enzyme 5-lipoxygenase (5-LOX), one of the most physiologically important lipoxygenases (Giribaldi et al., 1993; Chen et al., 1998), produces LTs, that are formed during the decomposition of arachidonic acid (AA) through the LOX pathway (Koshihara et al., 1983; Shimizu et al., 1984; Pontiki et al., 2011), and have been implicated in the pathogenesis of disorders associated with inflammation, for example, asthma and allergic rhinitis, and have become major targets for therapeutic modulation (Busse, 1996).

The development of new and safe anti-inflammatory agents remains a subject of great interest (Gorzalczany et al., 2011). A group within the candidates for this type of research are specialised metabolites of plants used in folk medicine to treat inflammatory processes.

In this context, the present investigation focused in the chemical study of *L. caustica*, with the purpose of evaluating the activity of its specialised metabolites as inhibitors of 5-hLOX and 15-sLOX and correlating those results with *in silico* studies.

2. Results and discussion

2.1. Purification and analysis of epicuticular extract (dichloromethane extract)

The epicuticular extract of *L. caustica* (2.51 g), was fractionated by silica gel chromatography. Pure fractions after chromatography showed an intense dark blue spot when we used 10% FeCl3, indicating the presence of phenols. Finally, these fractions were regrouped and crystallized in methanol, yielding 0.342 g of a white solid and 0.193 g of an oil corresponding to the phenolic fraction, both of which were monitored by TLC and analyzed using 10% FeCl3.

To determine the complexity, proportion and purity of the epicuticular extract of the two products obtained, we used gas chromatography (GC) analysis. We observed a series of minor peaks between 10 and 30 min, but after 50 min, the most important signal appeared with purity of 90% (shown in Supplementary data).

With respect to GC of the solid, three major peaks were identified that were similar to the major peaks present in the epicuticular extract, showing a mixture of compounds of different molecular weights. On the other hand, the phenolic fraction exhibited a large signal at 52 min.

2.2. Chemistry

Characterization of the phenolic fraction was performed using spectroscopic techniques, such as IR-FT, GC-MS, 1H and 13C NMR (shown in Supplementary data). The IR-FT spectrum revealed a wide signal centered at 3441 cm-1, which was attributed to the HO stretching of hydroxyl groups, and a band was observed at the lower frequency of 3004 cm-1, which was attributed to the CH stretching of Csp 2-H bonds. The series of signals centered on 2953 cm-1, 2923 cm-1 and 2852 cm-1 were assigned to the C–H stretching of aliphatic groups. Finally, at a lower frequency, 1463 and 1277 cm-1 bands appeared, which were attributed to the C–O stretch present in the ring.

The chromatogram of the GC-MS analysis of the phenolic fraction showed a major peak at 38.5 min. The mass spectrum showed an M+ at 318 units of atomic mass (uma) consistent with formula C21H34O2 that has five unsaturated hydrocarbons. The base peak at m/z 123 ($C_7H_7O_2$) suggested a tropylium cation with two phenolic –OH groups (Fig. 2).

By GC-MS analysis, an alkylcatechol or an alkylresorcinol with an unsaturated hydrocarbon chain of 15 carbon atoms was predicted. The 1H and 13C NMR analysis of the phenolic fraction obtained from the epicuticular extract of *L. caustica* showed that the major compound corresponded to (*Z*)-3-(pentadec-10′-enyl)-catechol (1) (Fig. 3). From (*Z*)-3-(pentadec-10′-enyl)-catechol three synthetic derivatives: 3-pentadecylcatechol, 1,2-diacetyl-3-pentadecylbenzene, (*Z*)-1,2-diacetyl-3-(pentadec-10′-enyl)-benzene, were synthetized (See Supplementary data).

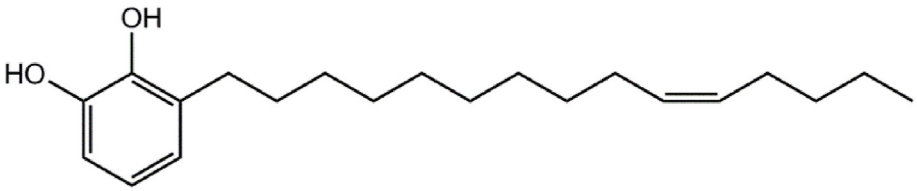

Fig. 3. (*Z*)-3-(pentadec-10′-enyl)-catechol structure.

2.3. 5- and 15-LOX inhibition, antioxidant and iron-reducing capacity, and enzymatic studies and docking

2.3.1. Inhibition of 15- and 5-LOX activity

Examination of the inhibitory activity of (*Z*)-3-(pentadec-10′-enyl)-catechol (**1**) against 5-hLOX was carried out using nordihydroguaiaretic acid (NDGA) as a positive control. The procedure was carried out by fluorimetry (Singh et al., 2012) as described in more detail later in this section. For the determination of the IC50, different concentrations of the inhibitor were prepared using DMSO as the solvent. Biological studies showed a good and promissory IC50 (2.09 μM), but not comparable to good and known 5-hLOX inhibitors (Singh et al., 2012), such as zileuton, atreleuton and NDGA, with IC_{50} values between 0.32, 0.08 and 0.02 μM, respectively. Furthermore, zileuton, an iron chelator (Nair and Funk, 2009), is the only drug approved by the Food and Drug Administration (FDA) for psoriasis treatment.

To determine whether (*Z*)-3-(pentadec-10′-enyl)-catechol (**1**) is a specific inhibitor of 5-hLOX, we decided to examine with other LOX isoform, 15-sLOX (shown in Supplementary data). The 15-sLOX enzyme was taken as a study model because, although the human enzyme is also commercially available, it is less stable than that of plant origin, exhibiting low biological activity by *in vitro* studies. The alignment of the sequences of human and soybean 15-LOX yielded a 28% identity. Although this could be taken as an indication of little identity between the two isoforms, a comparative study of their active sites showed that all residues that are part of the binding site, and that interact with the AA and iron (Wecksler et al., 2009), are highly conserved in both systems, being the 15-sLOX a first good model for studying human 15-LOX inhibitors.

The IC50 value obtained for 15-sLOX was 54.77 μM, which is less potent than previously reported inhibitors, such as baicalein (35 μM) or kaempferol (50 μM) (Sadik et al., 2003). When we compared the IC50 values obtained for both enzymes, 5-hLOX (2.09 μM) and 15-sLOX (54.77 μM), the (*Z*)-3-(pentadec-10′-enyl)-catechol (**1**) showed to be a potent and selective inhibitor of 5-hLOX compared to 15-sLOX. One possible explanation for this discrepancy may be differences in the size of the active sites for both enzymes, as the 5-hLOX active site is 20% larger than the 15-sLOX active site (Gillmor et al., 1997) and the their analysis of sizes of cavities in both enzymes, allowing give the structural explications about as the 5th or 15th carbons of the arachidonic acid are placed in front to metal and beginning the catalytic cycle.

Analysis of the (*Z*)-3-(pentadec-10′-enyl)-catechol (**1**) structure and its relationship to 5-LOX inhibition revealed two keys factors: the catechol group, that would affect the potency against 5-LOX and the alkyl chain (Peduto et al., 2017). For this, three derivatives were synthesized, two of which block the catechol group through acetylation as compounds (**3**) and (**4**) and one with saturated side chain (**2**). Table 1 shows the average values of 5-hLOX activities in the presence of the different synthetic derivatives. The main results showed that blocking the catechol group of (*Z*)-3-(pentadec-10′-enyl)-catechol (**1**) using acetyl groups dramatically decreased inhibition, but this difference was not observed when we reduced the double bond through catalytic hydrogenation. In parallel, we made the same comparison but with 15-sLOX. The IC_{50} showed that (*Z*)-3-(pentadec-10′-enyl)-catechol (**1**) (54.77 μM) and 3-pentadecylcatechol (**2**) (55.28 μM) did not exhibit dramatic decreases of inhibition whether we used the unsaturated chain or not, unlike what we observed in 5-hLOX, as was demonstrated comparing other types of systems in previous research (Sugiura et al., 1989; Schaible et al., 2016). These differences could be due to different inhibitory mechanisms between LOX isoforms.

Table 1
Percent inhibition of the enzyme 5-hLOX with respect to antioxidant and reductive capacity as measured by the DPPH, ABTS and FRAP methods. Values of maximum speed (Vmax), Michaelis constant (K_m) and inhibition constant (K_i) are also shown for (*Z*)-3-(pentadec-10′-enyl)-catechol (**1**) and 3-pentadecylcatechol (**2**).

Screening inhibitory activity of 5-hLOX						
		(1)	(2)	(3)	(4)	NDGA
% Inhibition		69.6	79.4	NA	NA	96.7
		73.7	76.3	NA	NA	95.1
		63.1	73.9	NA	NA	88.7
Inhibition average		68.8	76.6	NA	NA	93.5
SD		± 5.3	± 2.7	–	–	± 4.2
Antioxidant and iron-reducing capacity						
Assays		(1)	(2)	(3)	(4)	Background
DPPH	% free radicals	16.7	16.2	90.0	89.5	100
	% entrapment	83.3	83.8	9.9	10.5	0
ABTS	% free radicals	10.2	10.1	75.1	74.4	100
	% entrapment	89.8	89.9	24.9	25.6	0
FRAP	Antioxidant capacity/Iron-reducing (μg/mL)	33.61	45.34	4.84	4.34	–
Enzymatic kinetics						
Inhibitor	(2)				(1)			
[I] μM	0	0.5	1.5	3	0	0.5	1.5	3
V_{max}	1949	1242	1042	944.7	1435	1280	1025	794
Km	36.9	73.6	87.3	111	33.8	78.3	84.8	95.9
$K_{i\ app}$ (μM)	0.33 (Mixed Mechanism)				0.95 (Mixed Mechanism)			
	K_i (0.14)				K_i (0.40)			
	$K_{i'}$ (0.71)				$K_{i'}$ (1.95)			

2.3.2. Antioxidant activity

Due to the results described above and the importance of catechol to 5-hLOX inhibition, three different methods to estimate antioxidant activity were performed. DPPH evaluates antioxidant activity using the free radical 2,2-diphenyl-1-picrylhydracil (DPPH), which determines radical capture in the presence of an antioxidant substance by spectrophotometry at 520 nm. ABTS is based on quantification of the discoloration of the radical ABTS • + due to interaction with donor species of hydrogens or electrons. The cationic radical ABTS • + is a chromophore that absorbs at 734 nm and is generated by an oxidation reaction of ABTS (2,2′-azino-bis-(3-ethyl benzthiazolin-6-sulfonate ammonium) with potassium persulfate. In contrast, FRAP measures the antioxidant capacity of a sample based on its ability to reduce the ferric iron Fe (III) present in 2,4,6-tri-(2-pyridyl)-s-triazine (TPTZ) to the ferrous form Fe (II) and has a maximum absorbance at a wavelength between 590 and 595 nm. The results are shown in Table 1.

Table 1 shows that the compounds with the highest antioxidant capacity, according to the DPPH and ABTS assays, were 3-pentadecylcatechol (**2**) and (*Z*)-3-(pentadec-10′-enyl)-catechol (**1**), which were the two compounds with catechol groups in their structure. Replacing the catechol groups with diacetylated derivatives (**3**) and (**4**) decreased the antioxidant capacity considerably. The FRAP experiments

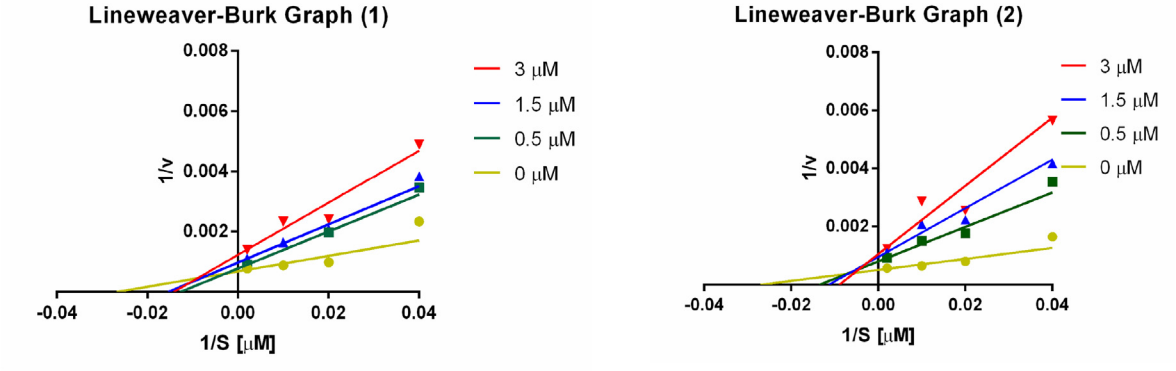

Fig. 4. (*Z*)-3-(pentadec-10′-enyl)-catechol (**1**) and 3-pentadecylcatechol (**2**) Lineweaver-Burk graphs.

demonstrated the same behavior, and compounds that had greater antioxidant properties or iron-reducing capacities were the compounds with a catechol group in their structure. These results are in agreement with the IC_{50} experiments described above.

2.3.3. Kinetic experiments

Based on our results, we next investigated the type of inhibition by (*Z*)-3-(pentadec-10′-enyl)-catechol (**1**) and 3-pentadecylcatechol (**2**) against 5-hLOX using enzyme kinetics. The enzyme 5-hLOX has iron as a central atom, and when in the ferric state Fe (III), the enzyme is catalytically active, while in its ferrous state Fe (II), the enzyme is inactive. To determine the mechanism of inhibition by (**1**) and (**2**) against 5-hLOX, an examination of the enzymatic kinetics was carried out to determine the binding characteristics of these compounds with the enzyme. The appropriate kinetics parameters as V_m, K_m and K_i were obtained directly from *v* and *s* values without any transformation to a reciprocal by Michaelis-Menten. The representation of the respective inhibition mechanisms were obtained for (**1**) and (**2**) by kinetics experiments as we shown in Fig. 4. In both cases, the same behaviors were observed, a decrease V_m and a change in K_m, as results the $K_{i\ app}$, were 0.95 and 0.33 μM respectively, suggesting a mixed mechanism of inhibition in both compounds. These results represent that the inhibitor can bind to the free enzyme (competitive) and to the ES complex (uncompetitive). The analysis to the $K_{m,\ app}$ in (**1**) and (**2**), indicated that the compound (**1**) had a higher preference for competitive mechanism ($K_{m,\ app} > K_m$) unlike to the uncompetitive preference of (**2**) ($K_{m,\ app} < K_m$).

2.3.4. Docking

We next performed *in silico* studies to understand the binding mode for the two most potent and selective inhibitors. The first study localized the binding site of ligands by docking using the crystal structure of 5-hLOX (PDB ID 3O8Y) at a resolution of 2.30 Å. The results revealed that all ligands were in the active site but exhibited differential affinities. For example, the ΔG value obtained for the ligand (**1**) (−5.55 kcal/mol) was comparable in affinity and energy to (**2**) (−5.07 Kcal/mol), demonstrating two principal interactions with the residues ILE-637 and ASN-407 by hydrogen bonding with the catechol group oriented in front of the iron at a distance of approximately 2.5 Å. Finally, the binding energies detected for the acetylated derivatives (**3**) and (**4**) were +7.66 Kcal/mol and +7.78 Kcal/mol, respectively.

We observed that (**1**) and (**2**) oriented the catechol group towards the metallic center. This characteristic, together with the results obtained from the iron reducing capacity (FRAP), DPPH and ABTS in Table 1, suggest a redox inhibition that comprises a mixed mechanism identified by enzyme kinetics.

2.3.5. Molecular dynamics

To determine the importance of the catechol groups, present in (**1**) and (**2**) and to correlate our biological and antioxidant experiments, we carried out molecular dynamics simulations (MD) with 5-hLOX. The analysis of MD simulations showed that the compound (**2**) interacted with the residue ASN-407 through donor hydrogen bonding. Furthermore, we observed that the catechol group initially tended to move away from the metallic center, with an average maximum distance of 4.3 Å and a minimum at 2.8 Å at 10 ns of MD. The same behavior was observed with the compound (**1**), and the main interaction found was with ASN-407 as we showed with (2), with the minimum average distance at 3.7 Å.

Following our MD study and the mixed mechanism determined by kinetic experiments, we next performed MD using the substrate arachidonic acid (AA) and the best inhibitors, (**1**) and (**2**) found. The results demonstrated that in the first system (**Complex 2-AA**), the molecules were positioned near the binding site, with the principal interaction occurring between the derivate (**2**) and ASN-407, which placed the catechol group very close to the metal. Meanwhile, AA interacted with THR-364, HIS-432, GLN-557, GLN-363 and THR-427, as has been previously described in the literature (Gillmor et al., 1997). Fig. 5A shows the distance between the catechol group and the iron with a change along the simulation time. In an initial state, the average distance was 6.8 Å, but during and at the end of the MD we observed that the catechol slowly approached at a distance of 5.4 Å, and AA placed C-7 of the hydrocarbon chain in front of the metal during the initial state of MD. These results show a slight preference to the enzyme for the substrate compared with the derivate (**2**). Similar simulations were done by MD, between AA and the molecule (**1**) (Fig. 5B), the fluctuation of the distance between the catechol group and iron was 4.4 Å at 3.5 Å, indicating the higher affinity to the inhibitor than the substrate to 5-hLOX. Finally, both results obtained for the compounds (**1**) and (**2**) by MD they were agree with the mixed mechanism obtained by enzymatic assays.

3. Conclusions

The (*Z*)-3-(pentadec-10′-enyl)-catechol (**1**) was evaluated for the first time against LOX isoforms, revealing significant inhibition of enzymatic activity for two enzymes (15-sLOX, IC_{50} 54.77 μM; 5-hLOX, IC_{50} 2.09 μM), demonstrating that it is a relatively specific inhibitor of 5-hLOX. In addition, the enzymatic activity of the reduction product of (*Z*)-3-(pentadec-10′-enyl)-catechol (**1**), 3-pentadecylcatechol (**2**), and of the respective diacetylated derivatives, (*Z*)-1,2-diacetyl-3-(pentadec-10′-enyl)-benzene (**3**) and 1,2-diacetyl-3-pentadecylbenzene (**4**), were determined, demonstrating that the presence of a catechol group in this type of system is essential for the inhibition of 5-hLOX and not the unsaturated chains.

Through enzyme kinetics studies, it was determined that (*Z*)-3-(pentadec-10′-enyl)-catechol (**1**) and 3-pentadecylcatechol (**2**) were potent and selective inhibitors the 5-hLOX and a mixed inhibition

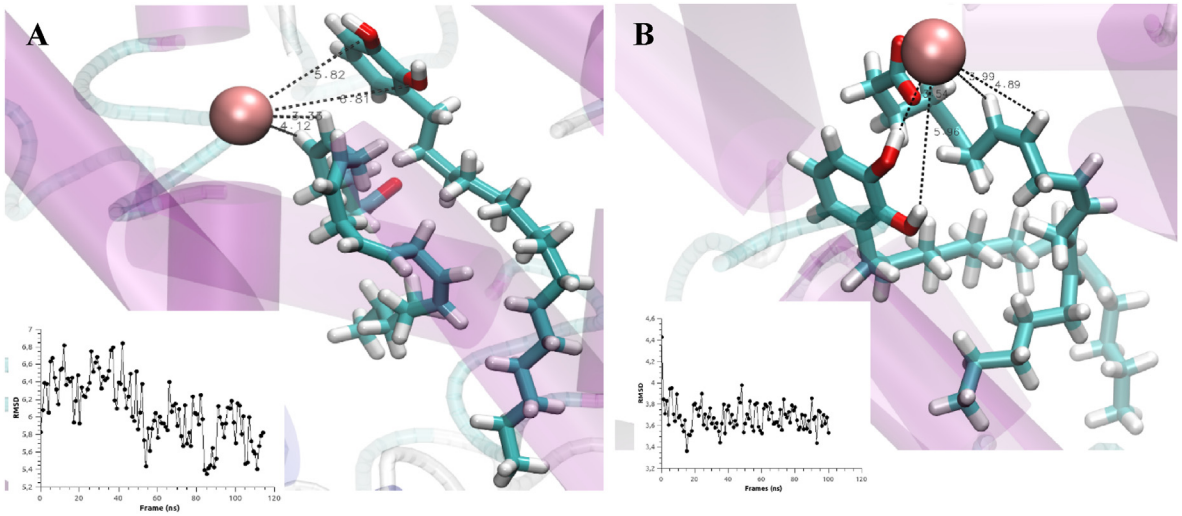

Fig. 5. Active site of molecular dynamics between 3-pentadecylcatechol (**2**) (A), (*Z*)-3-(pentadec-10′-enyl)-catechol (**1**) (B), and arachidonic acid with 5-hLOX and fluctuation of catechol distances during simulation time (10 ns).

mechanism with a K_i of 0.95 μM for (*Z*)-3-(pentadec-10′-enyl)-catechol (**1**) and 0.33 μM for 3-pentadecylcatechol (**2**) were obtained, which was confirmed by MD simulations.

4. Experimental

4.1. Plant material

Leaves of *Lithrea caustica* (Molina) Hook and Arn. (Anacardiaceae) were collected during the flowering season, Abril 2017, in Farellones, Santiago Metropolitan Region, Chile (33° 18′ 35.9″S; 70° 19′ 19.9″W) at altitudes of 1200–1300 m above sea level (masl). Voucher specimens (SGO-067800) were deposited in the Herbarium of the National Museum of Natural History, Santiago, Chile.

4.1.1. Extraction of epicuticular resin with dichloromethane. Epicuticular extract

Fresh leaves of *L. caustica* (1.4 kg) were placed in 1 L beaker and dichloromethane was added to cover the volume of the leaves (final volume 5 L), which were macerated for 5 min by stirring with a glass rod. Next, the solution was filtered, and the dichloromethane was eliminated under reduced pressure in a rotary evaporator. Finally, the extract was stored in the dark at 5 °C, yielding (6.1 g, 0.44%).

4.2. Chemistry

4.2.1. Gas-liquid chromatography analysis of epicuticular extract and isolated compounds

The epicuticular extract and isolated compounds from *L. caustica* were analyzed by GLC using a Shimadzu GC-2010 Plus equipped with an HP-5 column (30 m × 0.250 mm x 0.25 μm), samples (10 mg/mL) were prepared in dichloromethane. The chromatogram was developed using a thermal gradient as follows: 5 min at 40 °C, 10 °C/min to 200 °C, 5 min at 200 °C; 3 °C/min to 300 °C, 20 min at 300 °C.

4.2.2. IR-FT, ^{1}H and ^{13}C NMR analysis

The IR-FT spectra of (*Z*)-3-(pentadec-10′-enyl)-catechol (**1**), 3-pentadecylcatechol (**2**), (*Z*)-1,2-diacetyl-3-(pentadec-10′-enyl)-benzene (**3**) and 1,2-diacetyl-3-pentadecylbenzene (**4**) were imaged on film using a PerkinElmer Spectrum 65, and ^{1}H and ^{13}C NMR spectra were recorded on a Bruker Advance 400 (400 MHz) (shown in Supplementary data).

4.3. Procedure for synthesis of 3-pentadecylcatechol (2)

To a solution of (*Z*)-3-(pentadec-10′-enyl)-catechol (**1**) (0.88 mmol) in 20 mL methanol, 10% catalyst Pd/C was added. The reaction was carried out in a reactor at 2 bar of hydrogen pressure stirring for 4 h at room temperature. The product was then filtered and washed with methanol. Physical and NMR data are listed below:

4.3.1. (Z)-3-(pentadec-10′-enyl)-catechol (1)

Yield 8%; oil. 1H NMR (CDCl3, 400 MHz, δ, ppm) δ: 6.71 (s, 3H, CH); 5.36 (t, 2H, JH-H = 4.5 Hz, CH); 2.60 (t, 2H, JH-H = 7.6 Hz, CH2); 2.02 (m, 2H, CH2); 1.40–1.26 (m, 18H, CH2); 0.90 (t, 3H, JH-H = 6.6, CH3). 13C NMR (CDCl3, 400 MHz, δ, ppm) δ: 143.0 (s, C); 141.9 (s, C); 129.9 (s, CH); 129.8 (s, CH); 129.3 (s, C); 122.0 (s, CH); 120.0 (s, CH); 112.8 (s, CH); 31.9 (s, CH2); 29.8–29.4 (m, 7C, CH2); 29.3 (s, CH2); 27.2 (s, CH2); 26.9 (s, CH2); 22.3 (s, CH2); 14.0 (s, CH3).

4.3.2. 3-Pentadecylcatechol (2)

Yield 62%; solid, 1H NMR (CDCl3, 400 MHz, δ, ppm) δ: 6.71 (s, 3H, CH); 2.60 (t, 2H, JH-H = 7.8 Hz, CH2); 1.26 (m, 26H, CH2); 0.89 (t, 3H, JH-H = 6.5, CH3). 13C NMR (CDCl3, 400 MHz, δ, ppm) δ: 143.5 (s, C); 142.4 (s, C); 129.8 (s, C); 122.4 (s, CH); 120.4 (s, CH); 113.2 (s, CH); 32.3 (s, CH2); 30.2–29.8 (m, 12C, CH2); 23.1 (s, CH2); 14.5 (s, CH3).

4.4. General procedure for synthesis of diacetylated derivatives

To a solution of alkyl catechol (0.19 mmol) in 8 mL CH_2Cl_2, 2.22 mmol acetic anhydride and 4-dimethylaminopyridine (0.20 mmol) were added. The mixture was stirred for 24 h at room temperature. Next, the solution was washed with 5% HCl, followed by 6% $NaHCO_3$ and finally with water. After washing, the solution was dried using anhydrous sodium sulfate, then filtered and evaporated. Physical and NMR data are listed below:

4.4.1. (Z)-1,2-diacethyl-3-(pentadec-10′-enyl)-benzene (3)

Yield 71.8%; oil. 1H NMR (CDCl3, 400 MHz, δ, ppm) δ: 7.86 (d, 1H, JH-H = 7.5 Hz, CH); 7.68 (t, 1H, JH-H = 8.2 Hz, CH); 7.31 (d, 1H, JH-H = 8.2 Hz, CH); 5.35 (t, 2H, JH-H = 4.7 Hz, CH); 2.51 (t, 2H, JH-H = 7.6 Hz, CH2); 2.31 (s, 3H, CH3); 2.27 (s, 3H, CH3); 2.02 (m, 2H, CH2); 2.01 (m, 2H, CH2); 1.33–1.26 (m, 18H, CH2). 13C NMR (CDCl3, 400 MHz, δ, ppm) δ: 168.7 (s, C=O); 168.6 (s, C=O); 142.8 (s, C); 140.9 (s, C); 137.1 (s, C); 130.2 (s, CH); 129.9 (s, CH); 127.6 (s, CH); 126.5 (s, CH); 121.2 (s, CH); 32.3 (s, CH2); 31.9 (s, CH2); 30.4–29.6 (m,

7C, CH2); 27.5 (s, CH2); 27.3 (s, CH2); 22.7 (s, CH2); 21.1 (s, CH3); 20.7 (s, CH3); 14.3 (s, CH3).

4.4.2. 1,2-Diacethyl-3-pentadecylbenzene (**4**)

Yield 82.4%; solid. 1H NMR (CDCl3, 400 MHz, δ, ppm) δ: 7.18 (d, 1H, JH-H = 6.9 Hz, CH); 7.12 (t, 1H, JH-H = 7.6 Hz, CH); 7.04 (d, 1H, JH-H = 8.0 Hz, CH); 2.51 (t, 2H, JH-H = 7.6 Hz, CH2); 2.31 (s, 3H, CH3); 2.27 (s, 3H, CH3); 1.26 (m, 26H, CH2); 0.88 (t, 3H, JH-H = 6,4 Hz, CH3). 13C NMR (CDCl3, 400 MHz, δ, ppm) δ: 168.7 (s, C=O); 168.6 (s, C=O); 142.8 (s, C); 140.9 (s, C); 137.1 (s, C); 127.6 (s, CH); 126.5 (s, CH); 121.2 (s, CH); 32.3 (s, CH2); 30.5–29.7 (m, 12C, CH2); 23.1 (s, CH2); 21.1 (s, CH3); 20.7 (s, CH3); 14.5 (s, CH3).

4.5. Determination of the inhibitory activity of (Z)-3-(pentadec-10′-enyl)-catechol (**1**), 3-pentadecylcatechol (**2**), (Z)-1,2-diacetyl-3-(pentadec-10′-enyl)-benzene (**3**) and 1,2-diacetyl-3-pentadecylbenzene (**4**) against soybean 15-lipoxigenase (15-sLOX)

Analysis of 15-sLOX activity (Cayman Chemical Item Nº. 60,712) was performed at 234 nm (ε = 25.000 $M^{-1}cm^{-1}$) and was produced due to the formation of the conjugated diene, which was measured using a Perkin spectrophotometer-Elmer Lambda 25 UV/Vis. All reactions were carried out with a final volume of 2 mL with constant agitation at room temperature. For this reaction, a 0.1 M HEPES buffer was prepared at pH 7.4 containing Triton X-100 and 10 μM of the linoleic acid substrate. IC_{50} values were determined using the GraphPad Prism Demo v 8.2.1.

4.6. Determination of the inhibitory activity of (Z)-3- (pentadec-10′-enyl)-catechol (**1**), 3-pentadecylcatechol (**2**), (Z)-1,2-diacetyl-3- (pentadec-10′-enyl)-benzene (**3**) and 1,2-diacetyl-3-pentadecylbenzene (**1**) against human 5-lipoxygenase (5-hLOX) using enzyme kinetics assays

This fluorescence-based assay is performed using microplates. The enzyme (Cayman Chemical Item No. 60402) was diluted (1:500) in the assay buffer (HEPES 50 mM, EDTA 2 mM, ATP 10 μM and $CaCl_2$ 10 μM at pH 7,5) and mixed with 10 μM of H2DCFDA dye. The reaction mixture was incubated for 15 min in the assay plate. Subsequently, 280 μL of assay buffer was added per well, and 10 μL of inhibitor was added to a final concentration of 10 μM; this reaction mixture was incubated for 30 min. The reaction was started by the addition of a suitable concentration of arachidonic acid (0.5 μM), and fluorescence was read in a multimode detector Synergy™ HT Multi-Mode Microplate Reader (Biotek) at 480 nm excitation/520 nm emission after a reaction that had proceeded for 1 h at room temperature for determinate the %I values. The IC_{50} values were obtained by the same procedure describe above but with different inhibitor concentrations (0–10 μM). Finally, the kinetic assay was performed using different concentrations of substrate (0, 0.5, 1.5 and 3 μM) to determine the inhibitory mechanism and identify the best inhibitor under the experimental conditions described previously. All data were collected in duplicate, and the assays were performed on different days to ensure reproducibility of the methods used, the GraphPad Prism Demo v 8.2.1 was used for obtaining the corresponding IC_{50} (hyperbolic saturation curve) and kinetics parameters as (K_m, V_m) by nonlinear regression and K_i by double-reciprocal.

4.7. Evaluation of radical-trapping activity using DPPH

The assay for DPPH uptake capacity was performed in a 96-well microplate using 20 μL of 2.5 mg/mL compounds in methanol, which were added to 100 μL of 0.1 mM DPPH in methanol. The plate was incubated in the dark for 30 min at room temperature. The absorbance (A) of each reaction mixture was measured at 515 nm and compared with a blank methanol control using ascorbic acid as the calibration curve.

4.8. Evaluation of radical-trapping activity using ABTS

To prepare the reaction, sodium persulfate and ABTS were mixed with water. The compounds were allowed to react for 16 h and then were diluted by transferring 150 μL into 15 mL ethanol. Trolox (0–50 μM) was used for the calibration curve.

To measure the samples, 30 μL was added to 2000 μL ABTS reagent. The solution was allowed to stand for 7 min, and the absorbance was measured at 754 nm.

4.9. Evaluation of antioxidant activity by FRAP

To prepare the FRAP solution, 25 mL of 300 mM acetate buffer (pH 3.6) was mixed with 2.5 mL of 20 mM ferric chloride hexahydrate in distilled water, followed by the addition of 2.5 mL of 2,4,6-tris-(2-pyridyl)-s-triazine (TPTZ) 10 mM in 40 mM HCl. The samples were dissolved in methanol, and 1500 μl freshly prepared FRAP solution was added to each cuvette with 50 μL of the samples dissolved in methanol. The solution was allowed to stand for 4 min, and absorbance was measured at 593 nm using a PerkinElmer Lambda 25 UV/Vis spectrophotometer at room temperature.

4.10. Molecular modeling

The crystal structure of 5-hLOX was obtained from the Protein Data Bank database (PDB) website (http://www.rcsb.org/) in extension format *.pdb, code 3O8Y (resolution of 2.30 Å) containing an iron atom in the active site with Fe (III) oxidation state. From this file, the water molecules present in the macromolecule were eliminated. Using the AutoDockTools program, hydrogen atoms were added to the protein. Once these modifications were made, we proceeded to create a file with extension *. pdbqt, which contained the information generated from the partial charges and the types of atoms belonging to the macromolecule. Ligands were constructed using the GaussView 3.07 program, and geometric optimization was subsequently carried out using the Gaussian 09 program. For this optimization, the semi-empirical method (AM1) was initially used followed by the B3LYP method (6-31G*).

Once the structure was optimized and we had determined the partial charges derived from electrostatic potential (ESP), molecular coupling analysis was carried out using the Autodock 4 computer program and the Genetic-Lamarckian algorithm implemented by AutoDock with a size of grid of 100 points and the box centered on the nonhemic iron positioned in the catalytic site. Finally, a total of 100 runs were obtained.

Declaration of competing interest

The authors declare that they have no known competing financial interests or personal relationships that could have appeared to influence the work reported in this paper.

Acknowledgment

USA1799 – Vridei 021941 MC-PAP Universidad de Santiago de Chile. Postgraduate studies financed by CONICYT: CONICYT-PCHA/Doctorado Nacional/2014–21140089. Powered@NLHPC: This research/thesis was partially supported by the supercomputing infrastructure of the NLHPC (ECM-02).

Appendix A. Supplementary data

Supplementary data to this article can be found online at https://doi.org/10.1016/j.phytochem.2020.112359.

References

Alé, S.I., Ferreira, F., Gonzalez, G., Epstein, W., 1997. Allergic contact dermatitis caused by *Lithraea molleoides* and *Lithraea brasiliensis*: identification and characterization of the responsible allergens. Am. J. Contact Dermatitis 8, 144–149. https://doi.org/10.1016/S1046-199X(97)90094-4.

Aziz, M., Sturtevant, D., Winston, J., Collakova, E., Jelesko, J.G., Chapman, K.D., 2017. MALDI-MS imaging of urushiols in poison ivy stem. Molecules 22, 1–11. https://doi.org/10.3390/molecules22050711.

Busse, W.W., 1996. The role of leukotrienes in asthma and allergic rhinitis. Clin. Exp. Allergy 26, 868–879. https://doi.org/10.1111/j.1365-2222.1996.tb00621.x.

Chen, X., Reddanna, P., Reddy, G.R., Kidd, R., Hildenbrandt, G., Reddy, C.C., 1998. Expression, purification, and characterization of a recombinant 5-lipoxygenase from potato tuber. 243, 438–443. https://doi.org/10.1006/bbrc.1998.8115.

Diby, Y.B., Kone, M., Gbogbo, M., Yapo, A.P., 2016. Antidiarrhoeal properties of the ethyl acetate extract of the stem bark of *spondias mombin* L. (Anacardiaceae) in rats. World J. Pharm. Pharmaceut. Sci. 5, 387–397. https://doi.org/10.20959/wjpps20169-7673. Www.Wjpps.Com.

Gambaro, V., Chamy, M.C., von Brand, E., Garbarino, J.A., 1986. 3-(Pentadec-10-enyl)-catechol, a new allergenic compound from *Lithraea caustica* (Anacardiaceae). Planta Med. 52, 20–22. https://doi.org/10.1055/s-2007-969056.

Garro, M.F., Salinas Ibáñez, A.G., Vega, A.E., Arismendi Sosa, A.C., Pelzer, L., Saad, J.R., Maria, A.O., 2015. Gastroprotective effects and antimicrobial activity of *Lithraea molleoides* and isolated compounds against *Helicobacter pylori*. J. Ethnopharmacol. 176, 469–474. https://doi.org/10.1016/j.jep.2015.11.009.

Gillmor, S.A., Villaseñor, A., Fletterick, R., Sigal, E., Browner, M.F., 1997. The structure of mammalian 15-lipoxygenase reveals similarity to the lipases and the determinants of substrate specificity. Nat. Struct. Biol. 4, 1003–1009. https://doi.org/10.1038/nsb1297-1003.

Giribaldi, M.G., Basso, B., Righi, M., Bosisio, E., 1993. Potato lipoxygenase: a molecular biological approach. Pharmacol. Res. 27, 17–18. https://kundoc.com/pdf-potato-lipoxygenase-a-molecular-biological-approach-.html.

Gorzalczany, S., López, P., Acevedo, C., Ferraro, G., 2011. Anti-inflammatory effect of *Lithrea molleoides* extracts and isolated active compounds. J. Ethnopharmacol. 133, 994–998. https://doi.org/10.1016/j.jep.2010.11.031.

Gusinde, M., 1936. Plantas medicinales que los indios araucanos recomiendan. Anthropos 31, 555–873. https://doi.org/10.1016/j.celrep.2015.03.069.

Huang, C.Y., Kuo, C.H., Wu, C.H., Kuan, A.W., Guo, H.R., Lin, Y.H., Wang, P.K., 2018. Free radical-scavenging, anti-inflammatory, and antibacterial activities of water and ethanol extracts prepared from compressional-puffing pretreated mango (*Mangifera indica* L.) peels. J. Food Qual. 2018, 1–13. https://doi.org/10.1155/2018/1025387.

Imai, Y., Dobrian, A.D., Morris, M.A., Taylor-Fishwick, D.A., Nadler, J.L., 2016. Lipids and immunoinflammatory pathways of beta cell destruction. Diabetologia 59, 673–678. https://doi.org/10.1007/s00125-016-3890-y.

Kalergis, A.M., López, C.B., Becker, M.I., Díaz, M.I., Sein, J., Garbarino, J.A., De Ioannes, A.E., 1997. Modulation of fatty acid oxidation alters contact hypersensitivity to urushiols: role of aliphatic chain β-oxidation in processing and activation of urushiols. J. Invest. Dermatol. 108, 57–61. https://doi.org/10.1111/1523-1747.ep12285632.

Koshihara, Y., Neichi, T., Murota, S., Lao, A., Fujimoto, Y., Tatsuno, T., 1983. Selective inhibition of 5-lipoxygenase by natural compounds isolated from Chinese plants, *Artemisia rubripes* Nakai. FEBS Lett. 158, 41–44. https://doi.org/10.1016/0014-5793(83)80672-3.

Li, M.Y., Yuan, H.L., Ko, F.W.S., Wu, B., Long, X., Du, J., Wu, J., Ng, C.S.H., Wan, I.Y.P., Mok, T.S.K., Hui, D.S.C., Underwood, M.J., Chen, G.G., 2015. Antineoplastic effects of 15(S)-hydroxyeicosatetraenoic acid and 13- S -hydroxyoctadecadienoic acid in non-small cell lung cancer. Cancer 121, 3130–3145. https://doi.org/10.1002/cncr.29547.

López, C.B., Kalergis, A.M., Becker, M.I., Garbarino, J.A., De Ioannes, A.E., 1998. CD8+ T cells are the effectors of the contact dermatitis induced by urushiol in mice and are regulated by CD4+ T cells. Int. Arch. Allergy Immunol. 117, 194–201. https://doi.org/10.1159/000024010.

Montecino, S., Conejeros, A., 1985. Mujeres Mapuches, el saber tradicional en la curación de enfermedades comunes. Ser. Mujer y Salud. 88.

Nair, D.G., Funk, C.D., 2009. A cell-based assay for screening lipoxygenase inhibitors. Prostag. Other Lipid Mediat. 90, 98–104. https://doi.org/10.1016/j.prostaglandins.2009.09.006.

Nikolaev, V., Reddanna, P., Whelan, J., Hildenbrandt, G., Reddy, C.C., 1990. Stereochemical nature of the products of linoleic acid oxidation catalyzed by lipoxygenases from potato and soybean. Biochem. Biophys. Res. Commun. 170, 491–496. https://doi.org/10.1016/0006-291X(90)92118-J.

Peduto, A., Scuotto, M., Krauth, V., Roviezzo, F., Rossi, A., Temml, V., Esposito, V., Stuppner, H., Schuster, D., D'Agostino, B., Schiraldi, C., de Rosa, M., Werz, O., Filosa, R., 2017. Optimization of benzoquinone and hydroquinone derivatives as potent inhibitors of human 5-lipoxygenase. Eur. J. Med. Chem. 127, 715–726. https://doi.org/10.1016/j.ejmech.2016.10.046.

Perrotta, V.G., Arambarri, A.M., 2004. Schinus longifolia var. longifolia (Anacardiaceae): anatomía foliar y caulinar. Acta Farm. Bonaerense 23, 142–147. http://hdl.handle.net/10915/6631.

Pontiki, E., Hadjipavlou-Litina, D., Litinas, K., Nicolotti, O., Carotti, A., 2011. Design, synthesis and pharmacobiological evaluation of novel acrylic acid derivatives acting as lipoxygenase and cyclooxygenase-1 inhibitors with antioxidant and anti-inflammatory activities. Eur. J. Med. Chem. 46, 191–200. https://doi.org/10.1016/j.ejmech.2010.10.035.

Russo, A., Cardile, V., De Ioannes, A., Garbarino, J., 2009. Effect of litreol on the viability of human cancer cells. Chem. Biol. Interact. 179, 178–184. https://doi.org/10.1016/j.cbi.2008.10.013.

Sadik, C.D., Sies, H., Schewe, T., 2003. Inhibition of 15-lipoxygenases by flavonoids: structure-activity relations and mode of action. Biochem. Pharmacol. 65, 773–781. https://doi.org/10.1016/S0006-2952(02)01621-0.

San Martín, J., 1983. Medicinal plants in Central Chile. Econ. Bot. 37, 216–227. https://doi.org/10.1007/BF02858788.

Schaible, A.M., Filosa, R., Krauth, V., Temml, V., Pace, S., Garscha, U., Liening, S., Weinigel, C., Rummler, S., Schieferdecker, S., Nett, M., Peduto, A., Collarile, S., Scuotto, M., Roviezzo, F., Spaziano, G., de Rosa, M., Stuppner, H., Schuster, D., D'Agostino, B., Werz, O., 2016. The 5-lipoxygenase inhibitor RF-22c potently suppresses leukotriene biosynthesis in cellulo and blocks bronchoconstriction and inflammation in vivo. Biochem. Pharmacol. 112, 60–71. https://doi.org/10.1016/j.bcp.2016.04.019.

Shimizu, T., Radmark, O., Samuelsson, B., 1984. Enzyme with dual lipoxygenase activities catalyzes leukotriene A_4 synthesis from arachidonic acid. Proc. Natl. Acad. Sci. U.S.A. 81, 689–693. https://doi.org/10.1073/pnas.81.3.689.

Singh, R.K., Gupta, S., Tiwari, P., Saini, S., Malik, R., Kant, R., Dasditar, S.G., Ray, A., 2012. A fluorescent based enzyme assay for recombinant human lipoxygenase enzyme isoforms. Pharmacologia 3, 387–396. https://doi.org/10.5567/pharmacologia.2012.387.396.

Sugiura, M., Naito, Y., Yamaura, Y., Fukaya, C., Yokomaya, K., 1989. Inhibitory activities and inhinibition specificities of caffeic acid derivatives and related compounds toward 5-lipoxygenase. Chem. Pharm. Bull. 37, 1039–1043. https://doi.org/10.1248/cpb.37.1039.

Teillier, S., Villaseñor, R., Marticorena, A., Novoa, P., Niemeyer, H., 2018. Flora del litoral de la región de Valparaíso. Productora gráfica Andros Ltda, Santiago, Chile.

Urzúa, A., Sotes, G., Echeverría, J., 2011. Presence of 3-(pentadec-10-enyl)-catechol allergen in the epicuticular components of *Lithrea caustica* (Anacardiaceae). Bol. Latinoam. y Del Caribe Plantas Med. y Aromat. 10, 590–594. http://www.scopus.com/inward/record.url?eid=2-s2.0-83055164475&partnerID=40&md5=5c93ea6ed7496486c2fd6e1f9eb8ff1b.

Wecksler, A.T., Garcia, N.K., Holman, T.R., 2009. Substrate specificity effects of lipoxygenase products and inhibitors on soybean lipoxygenase-1. Bioorg. Med. Chem. 17, 6534–6539. https://doi.org/10.1016/j.bmc.2009.08.005.

Yar, M., Sidra, L.R., Pontiki, E., Mushtaq, N., Ashraf, M., Nasar, R., Khan, I.U., Mahmood, N., Naqvi, S.A.R., Khan, Z.A., Shahzad, S.A., 2014. Synthesis, in vitro lipoxygenase inhibition, docking study and thermal stability analyses of novel indole derivatives: non-isothermal kinetic study of potent LOX inhibitor N'-(diphenylmethylene)-2-(1H-indole-3-yl) acetohydrazide. J. Iran. Chem. Soc. 11, 369–378. https://doi.org/10.1007/s13738-013-0308-3.